

Behaviour and Design of Steel I-Beam to Column End Plate Bolted Connections Based on Experimental and Numerical Investigations

A.H. Salem

Structural Engineering Dept., Ain Shams University, Egypt

E.Y. Sayed-Ahmed*

Construction Engineering Dept., the American University in Cairo, Egypt

A.A. Elserwi, R.S. Aziz

Structural Engineering Dept., Ain Shams University, Egypt

ABSTRACT: Steel Beam to column rigid connections are required to transfer forces and moments. I-beam are commonly connected to columns using bolted end plates rigid connections, which are mainly subjected to bending moment and shear force. Behaviour of these connections have been extensively investigated. However, besides being complicated, current methods of estimating bolt forces and plate thickness of the connections do not consider the interaction between the bolt elongation and the plate deformation. An experimental investigation is performed on rigid beam to column bolted connections with flushed and extended end plates. Then, a numerical model accounting for geometric and material nonlinearities is built up. The model results are verified against the experimental investigation data. Using this model, a parametric study is performed on the connection. Interaction curves have been presented, which reveals the effects of the investigated parameters on the bolts' forces, the prying action, the thickness of the end plate and the connection capacity. Modes of failure of these connections have been scrutinized showing two distinct modes: bolts failure or steel end plate yielding. The results of the investigation are used to perform a critical review of the procedures adopted by AISC for these rigid connections revealing the shortcomings of the AISC design procedures. Finally, design charts and equations for the rigid end plate connections are introduced based on the results of the experimental and numerical investigation, which may significantly facilitate the selection of both the bolt's diameters and the end plate thickness for the investigated connections.

1 INTRODUCTION

Rigid end plate beam to column connections are generally subjected to axial and shear forces in addition to bending moments. Behaviour and design of connections' bolts and their end plates have been extensively investigated (e.g. Mann 1968, Packer and Morris 1977, Krishnamurthy 1978, Tarpy and Cardinal 1981, Zoetemeijer 1981, Srouji et al. 1983, Sherbourne and Bahaari 1994, Bursi and Jaspert 1997, Coelho and Bijlaard 2007, Diaz et al. 2011, Wang et al. 2013, Ismail et al. 2014, Grimsmo 2015, Shi et al. 2017). Researchers aimed to enhance connection's design equations and scrutinize the effect of prying action on the bolt and the end plate. It was argued in these researches that pretensioned bolts increase the stiffness of the connection at levels of bending moment below its capacity. In connections with thick end plates, the influence of bolts pretensioning on early stiffness is more than that of a thin end plate. Based on these investigations, Murray and

Shoemaker (2002) introduced guidelines for design of flushed and extended end-plate moment connections, which is adopted by AISC guidelines no. 16. Despite all these extensive investigations, current methods of estimating bolt force and end plate capacity for rigid end plate connections are both complicated and do not consider the interaction between bolt elongation and end plate deformation.

This paper presents an experimental programme, which was conducted to investigate the behaviour of rigid connections subjected to pure bending moment. Connection specimens consist of two identical "beams" each ended with an end plate and an intermediate "column". The column is connected to the two beams using high strength bolts. Bolt used in the experimental investigation are M12 Grade 8.8 and M16 or M20 Grade 10.9; they were not pretensioned. Eight specimens were tested where they were divided equally into two groups: flushed and extended end plate connections. The material properties of the plates forming the beams, the columns

and the end plates were determined by three tension tests of coupons taken from the manufactured specimens. The bolts properties were determined by nine tests; three for each bolt diameter used.

Simple design charts and equations considering the interaction between the bolt force and the end plate deformation are introduced for the design of flushed and extended end plate connections. The developed charts and equations are based on the results of the experimental programme, which is also followed by an extensive numerical analysis performed on the said connection. The numerical model results were first verified against the outcomes of the current experimental programme and against the results of two other experimental programmes available from literature (Jenkins et al. 1986, Bose et al. 1996). Then, a parametric study is carried out using the numerical model in order to study the effect of different parameters on the connection behaviour. A comparative study between the investigation results and those obtained via the AISC design guide No. 16 provisions is also performed emphasizing the advantage of the proposed design method.

2 THE EXPERIMENTAL PROGRAMME

2.1 Connection Specimens and Test Set-up

An experimental programme has been conducted to investigate the behaviour of flushed and extended end-plate rigid connections subjected to pure bending moment. Details of the test setup are shown in Figure 1. The tested specimens consist of a “column” connected to two “beams” using high strength bolts. The two built-up section “beams” were used for all the tested connections (Figure 1). Each beam section is composed of two 200×20 mm flange plates and a 360×10 mm web plate, which produced a total beam’s height of 400 mm. Each beam was welded to a 30 mm stiffened head plate using 10 mm weld size. These dimensions and weld size ensure no beam deformation or weld failure during testing the connections. End plates 400×200 mm and 520×200 mm with different thicknesses were chosen to fit the flushed and extended connections, respectively for different bolt diameters and edge distances.

H-shaped “columns” composed of welded plates were used in the connection specimens as shown in Figure 1. Eight columns were fabricated for the tested connections. For flushed end plate connections, the column height and width were 440 mm and 300 mm, respectively with a 10 mm thick web plate. For extended end plate connections, only the column height was increased to 520 mm. Two 10 mm thick stiffeners were added to both sides exactly behind the beam flanges to prevent local deformation of the column flanges or web. All column flange plates were 440×200 mm. The horizontal edge distance to the outside edge of the plate was 50 mm.

The full length of the specimen is 3170 mm. The specimens were supported over two rollers which were placed on two IPEs 300 cross beams in order to simulate simply supported ends. In order to load the tested specimens with pure bending moment, a very rigid distributor beam was used under the hydraulic jack of the frame (Figure 1) with two cylinders added under the distributor beam, which were 680 mm apart. The locations of the two cylinders were designed to lie exactly over the stiffeners of the beams. This configuration distributed the load equally on both beams producing pure bending moment with no shear force on the tested connections.

Eight tests with the configurations shown in Figure 1 and Table 1 were performed with flushed and extended end plate connections which are denoted by F_n and E_n , respectively in Table 1. M12, M16 and M20 with Grades 8.8 and 10.9 non-pretensioned bolts were used in these connections with the configuration shown in Table 1 and Figure 1.

2.2 Steel and Bolts Properties

Two different types of bolts were used in the experimental programme: Grades 8.8 and 10.9. The mechanical properties of these bolt grades were determined by performing six direct tension tests on each bolt diameter: three tests were executed on bolts coupons, while the other three tests were conducted on bolts with heads and nuts as one unit. Thread was stripped for one of the tested M20 Grade 10.9 bolts with the other bolts tested with one or two nuts.

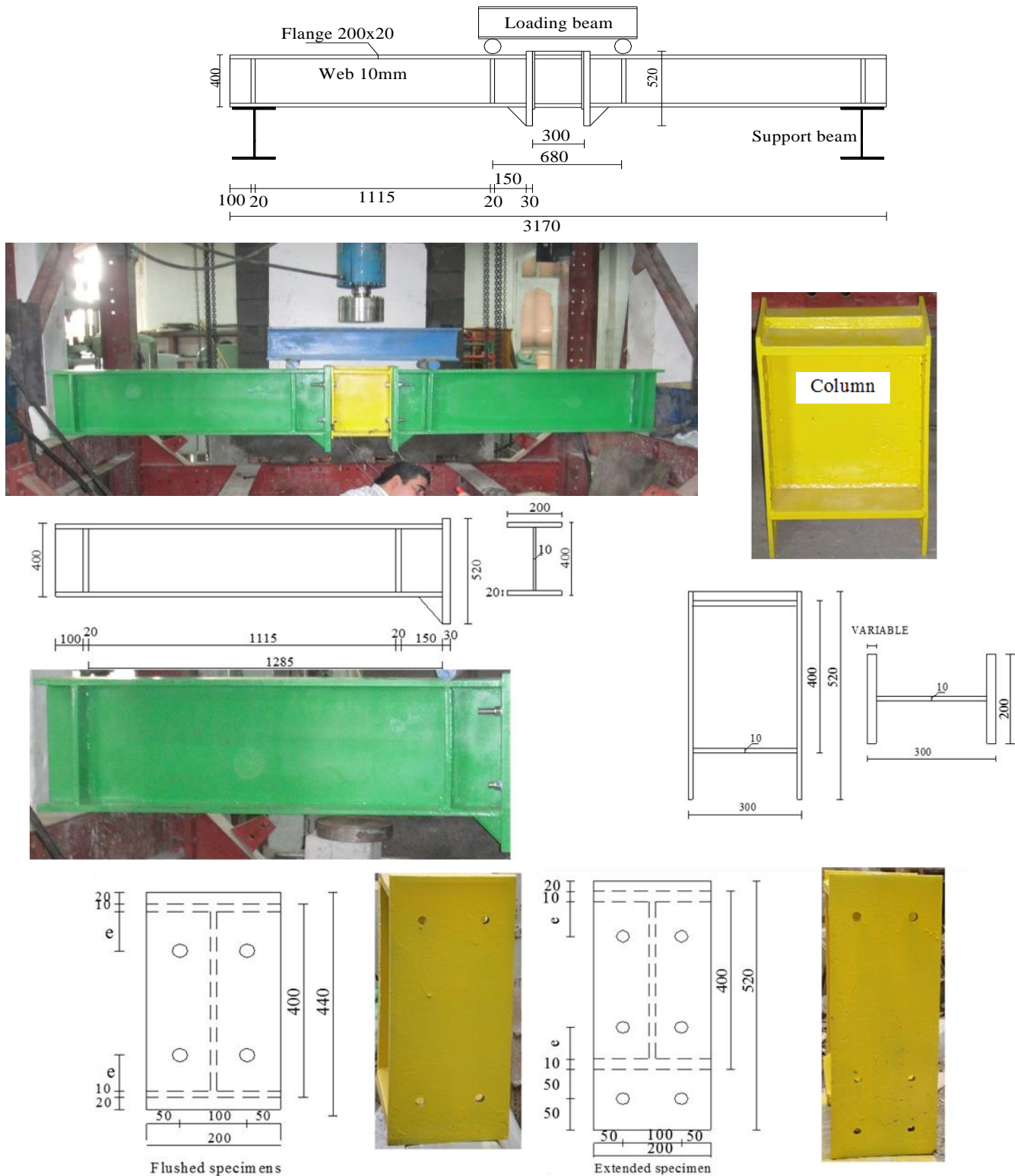


Figure 1. Test set-up and typical specimen of the tested connections.

In these tests, bolt rupture was always encountered, as expected, in the threaded part, which is the weakest and smallest bolt's section. Thus, the bolt area is commonly reduced at the threaded part by about 20%. Figure 2 and Table 2 shows the configurations and the results of these tests. It is evident from these tests that the bolt elongation at fracture ranges between 14% and 20%. Furthermore, all bolts revealed a 10% to 20% higher strength than its nom-

inal strength value. Thus, the ultimate strength of the M12, M16 and M20 bolts are considered to be 947 MPa, 1109 MPa and 1099 MPa, respectively.

The material properties of the component plates of beams, columns and end plates were derived by conducting standard tensile tests on three test coupons taken from the manufactured specimens. The tensile coupons were cut from each flat steel sheet (Figure 2) before preparing the connections.

Table 1. Configuration of the tested connection specimens.

Specimen name*	End plate Thickness (mm)	Bolt diameter and grade	Hole diameter (mm)	Edge distance (mm)
F1	20	M12 G8.8	14	40
F2	10	M20 G10.9	22	70
F3	10	M16 G10.9	18	70
F4	10	M12 G8.8	14	40
E1	20	M12 G8.8	14	40
E2	10	M20 G10.9	22	70
E3	10	M16 G10.9	18	70
E4	10	M12 G8.8	14	40

The size of the coupons and the test procedures follow ASTM-A370 specifications where $(12.5+0.25) \times (50+0.1)$ mm coupons were tested in uniaxial tension scheme to failure. Table 3 lists the results of the direct tension test performed on these steel coupons. From these tests, the steel yield and ultimate stress were found to be 274 MPa and 372 MPa, respectively. To evaluate the steel Young's modulus, some tensile coupons have been tested using extensometers. The modulus of elasticity of steel was found to be 206 GPa.



Figure 2. Direct tension testing of bolts and steel coupons.

Table 2. Results of testing the bolts in uniaxial tension.

a. Tests performed on bolts coupons								
Bolt	Spec No	Diameter before (mm)	Length before (mm)	Diameter after (mm)	Length after (mm)	Ultimate load (kN)	Ultimate stress (MPa)	Elongation %
M20	1	6	30	4.9	34.3	31.39	1120	14.3%
Grade	2	7	31	5.4	35.2	44.15	1159	13.5%
10.9	3	6.5	30.5	5.2	35	35.32	1080	15.1%
M16	1	6	30	5	34	30.41	1090	13.3%
Grade	2	6.5	30.5	5.2	35	35.32	1075	14.8%
10.9	3	6.5	31	5.4	35	36.30	1105	13%
M12	1	5	25	3.2	29.2	17.66	909	16.8%
Grade	2	5.5	25	3.9	30	23.54	1001	20%
8.8	3	5	26	3.4	30.3	18.64	959	16.53%

b. Tests performed on full bolts and nuts						
Bolt	Spec No	Number of nuts	Ultimate load (kN)	Ultimate* stress 1 (MPa)	Ultimate* stress 2 (MPa)	Failure mode
M20	1	1	245.25	788	985	Thread stripping
Grade	2	2	284.49	914	1143	Bolt rupture
10.9	3	2	299.21	961	1202	Bolt rupture
M16	1	1	166.77	837	1050	Bolt rupture
Grade	2	2	186.39	932	1169	Bolt rupture
10.9	3	2	178.54	896	1121	Bolt rupture
M12	1	1	93.20	832	1041	Bolt rupture
Grade	2	2	88.29	789	985	Bolt rupture
8.8	3	2	93.20	832	1041	Bolt rupture

*Ultimate stress 1 is based on the total area of the bolt, while ultimate stress 2 is based its effective area.

Table 3. Results of testing steel coupons of the steel used in the connection specimens.

Specimens	Coupon no.	P _u (kN)	P _y (kN)	t (mm)	b _{cu} (mm)	F _u (MPa)	F _y (MPa)	Elongation %
Flushed end plate connections	1	9.52	6.97	2.1	12.85	356	261	31.23
	2	9.71	7.16	2.0	12.75	385	283	32.27
	3	12.16	7.95	2.4	12.8	399	262	32.73
	Average					380	269	32.08
Extended end plate connections	1	13.73	10.30	3.0	12.3	376	281	35.52
	2	13.54	9.81	3.0	12.25	372	270	31.62
	3	11.58	8.44	2.5	12.65	370	270	34.54
	Average					373	274	33.89

2.3 Test Instrumentation

A load cell was used to record the applied load and dial gauges with an accuracy of 0.01 mm were used to measure the vertical displacement of the columns (Figure 3). Specimens were loaded incrementally at a loading rate of 9.81 kN/min (1.0 t/min) until failure took place. In order to catch the connection behaviour, small load intervals (1/20 of the expected connection capacity) were applied monotonically to failure. Each connection test lasted approximately half an hour to reach its ultimate load.

Vertical and horizontal electrical strain gauges were attached to the end plate in the expected locations of large deformation and prying action effect. For flushed end plate connections, two strains were attached between the bolt and the column flange and web (Figure 3). For the extended end plate connections, three strains were attached to each specimen at the locations shown in Figure 3. In order to measure the bolt strain and in turn the bolt force, an electrical

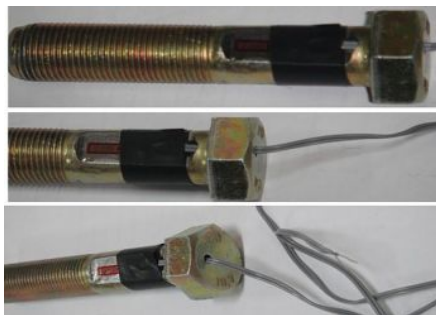
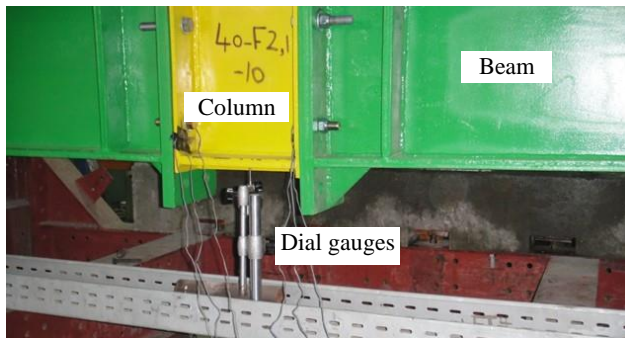
strain gauge was adhered to the shank part of the bolt as shown in Figure 3.

3 THE NUMERICAL MODEL

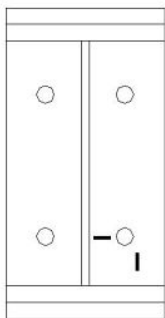
A numerical model (Figure 4) was built-up using ANSYS for a rectangular end plate welded to an I-beam and connected to an I-column by one or two rows of bolts at the tension side of the beam and by one row of bolts above the beam's compression flange to simulate connections with flushed end plates. Then, another model was built up for the same beam to column connection using two rows of bolts at the tension side of the beam and only one row of bolts above the beam's compression flange to simulate extended end plate connections.

Quadrilateral shell elements were used to model the beams, columns, stiffeners and end plates. Bolt head, nut and shank are modelled using eight-node solid elements. The nodes of bolt head and nut were

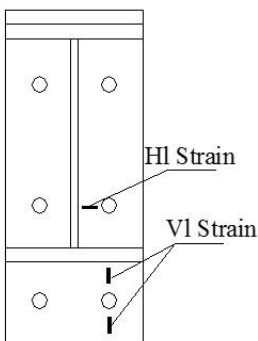
merged with those of the end plate and the column flange to ensure no separation during loading. Node-to-node contact elements were adopted to simulate contact and sliding between any two opposite nodes in the end plate and the column flange: each contact element has two nodes and three DOFs at each node and can withstand compression and Coulomb's friction in the contact's normal and tangential directions, respectively. This element does not transmit tension and it is completely separated if subjected to such stress.



Bolt's strain gauges



Flushed connection strain gauges



Extended connection strain gauges

Figure 3. Instrumentation and strain gauges for the tested connections.

The model considers both the geometric and the material nonlinearities. Full details of the numerical model are given elsewhere (Aziz 2010).

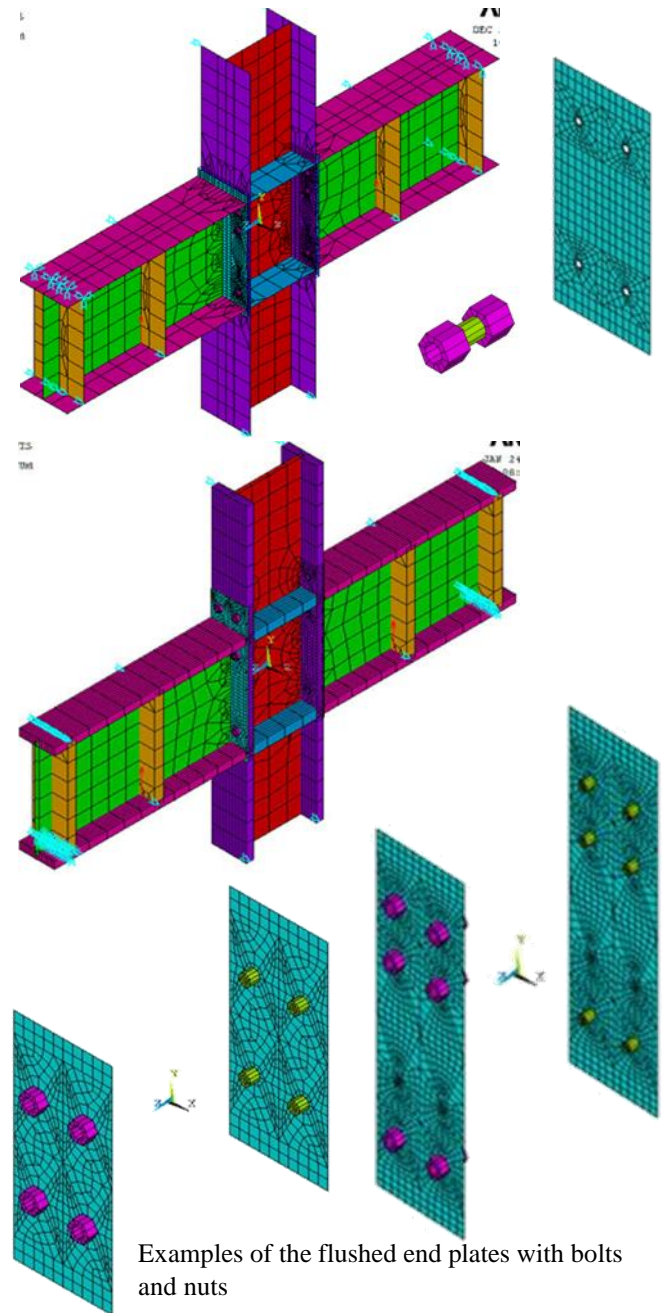


Figure 4. Finite element models of the flushed and extended end plate connections.

4 EXPERIMENTAL INVESTIGATION RESULTS AND VERIFICATION OF THE NUMERICAL MODEL

Ultimate loads and failure modes obtained from the numerical analysis and recorded during testing the connections are summarized in Table 1 and shown in Figures 5 and 6.

For extended end plate connections (Figure 5), Specimen E1 showed an excessive elongation in the

tension side bolts followed by bolt rupture. No deformation in the 20 mm thick column flanges was recorded. On the other hand, Specimen E2 showed a considerable flange deformation during loading. Bolts in the tension side of this specimen suffered from large rotation due to the end plate deformation, causing excessive stresses. Furthermore, this end plate deformed gradually due to a generated biaxial bending moments. Bolt prying appears in the two

positions: the lower end of the plate and end of the horizontal axis of the inner bolt. Specimen E3 showed the same behaviour of specimen E2, but with a different value for the failure load. In the same tested group, failure of Specimen E4 took place due to bolt failure associated with small end plate deformation.

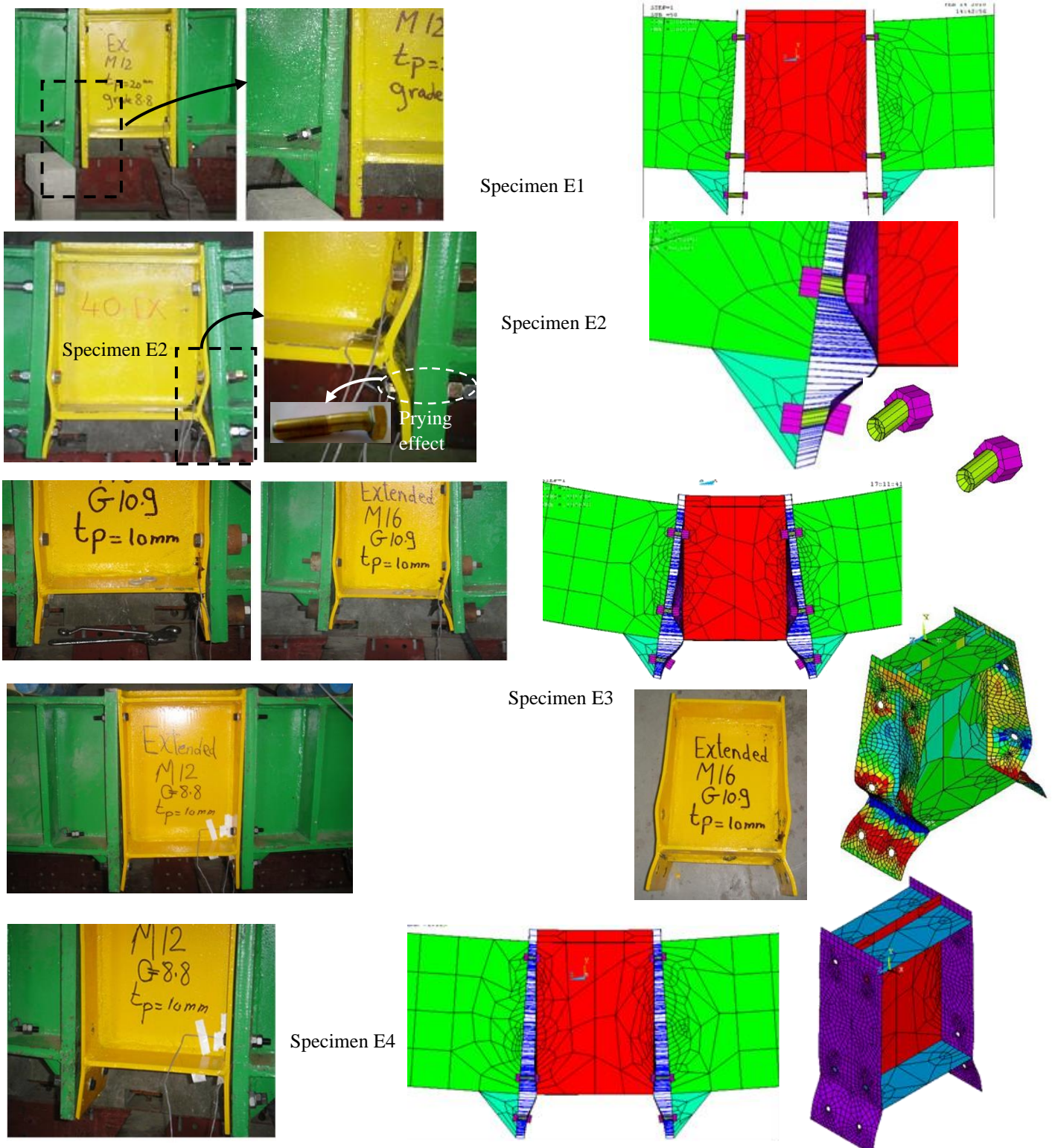


Figure 5. Failure modes of extended end plate connection specimens resulting from the numerical and experimental analyses.

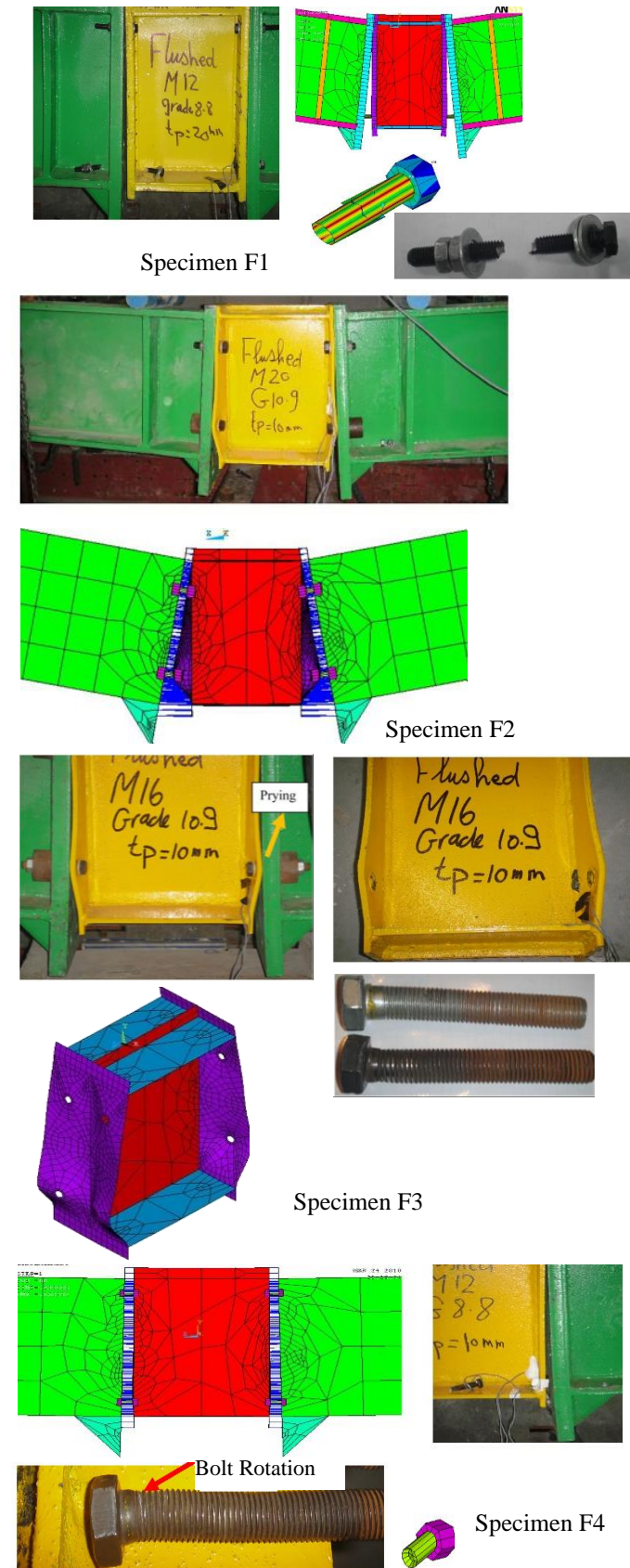


Figure 6. Failure modes of flushed end plate connection specimens resulting from the numerical and experimental analyses.

For flushed end plate connections (Figure 6), Specimen F1 showed an excessive elongation in the tension side bolts followed by bolt rupture; no deformation in the 20 mm thick column flanges was

recorded. Similar to Specimen E1, Specimen F2 showed a considerable flange deformation during loading. In this specimen, the plate deformed gradually due to biaxial bending moments, while the bolt prying force appears at the end of the horizontal axis of the inner bolt. The bolts in the tension side suffered from large rotations due to plate rotation causing excessive stresses. Specimen F3 showed the same behaviour as F2, but with a different value for the failure load. In specimen F4, failure also took place by bolt failure with small plate deformations; similar to the behaviour of Specimen E4.

It is evident from Figures 5 and 6, which compares the failure modes experimentally recorded and numerically predicted, that the finite element model was able to predict the behaviour of the tested connections. Table 4 also reveals a good agreement between the connection capacities recorded during testing all the specimens and obtained from the numerical analysis using the finite element model.

Figures 7 and 8 shows a comparison between end plate strains, bolts' strains and deflection measured experimentally and obtained numerically for two samples of the connections: F2 and E3. These figures also reveal the good agreement between the experimental results and the numerical analysis outcomes. Similar figures for the rest of the analysed connections are presented elsewhere (Aziz 2010).

The finite element model results have also been verified against connection specimens of other experimental investigations (Jenkins et al. 1986, Bose et al. 1996). The model outcomes only deviated by $\pm 7\%$ from these experimental results. Details of the later verification analyses along with mesh sensitivity analysis are given elsewhere (Aziz 2010).

5 THE PARAMETRIC INVESTIGATION

The finite element model is used to investigate the effect of different parameters on the capacity of extended and flushed end plate rigid connections. In this parametric investigation, stiffened and unstiffened end plate connections are considered.

A schematic drawing of the connections is shown in Figure 9. The column height is three times the height of the end plate. Thick plates for the column components are adapted to prevent local failure of column web or flanges, and to ensure that failure occurs in the bolts or the end plate. Stiffeners are added to prevent web crippling of the beam at the load and the support positions. Two loads are applied

(Figure 9) in order to generate a bending moment zone with no shear force at the connection's location. Roller support is considered at one side and hinged support at the other. Lateral supports are provided as shown in Figure 9 to prevent lateral displacement, side sway buckling of the column, and lateral torsion buckling of the beam's compression flange. The investigated parameters are

- End plate thickness “t” which is varied between 10 mm and 40 mm,
- Edge distance “e” of the bolt which is varied between 1.5 to 3.0 times the bolt diameter, and
- Bolt diameter “d” where M12 to M24 bolts are used in the analyzed connections.

High strength steel with a yield stress “F_y” of 353 MPa are adopted in for all analysed connections. In addition, Steel 24/35 and steel 28/44 are used for connections having M12 bolts and edge distance e = 1.5 d, and connections with M24 bolts and edge distance e = 3.0 d. This allows for investigating the effect of using a lower grade steel on the behaviour and moment capacity of the connections. Grade 10.9 bolts are used for all connections. In addition, Grade 8.8 bolts are used for connections having M12 and M24 bolts with edge distance e = 1.5 d.

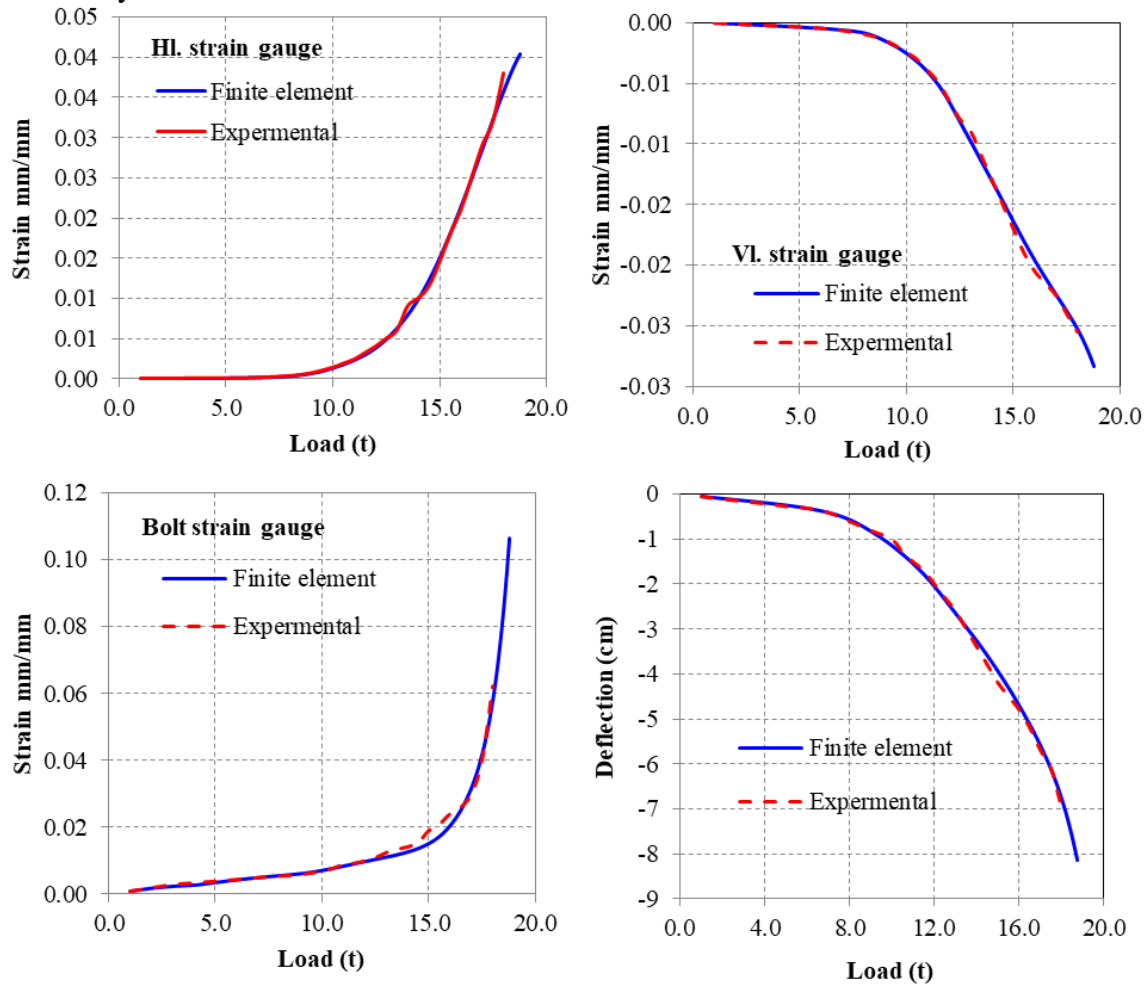


Figure 7. Comparisons experimental and numerical results for Specimen F2.

Table 4. Comparison between experimental and finite element model failure loads (mm)

Specimen	t _{End-plate} (mm)	Bolt dia. and grade	Hole dia. (mm)	Edge dist. (mm)	Exp. (kN)	FEM (kN)	FEM/Exp	Mode of failure
F1	20	M12 G8.8	14	40	138.32	156.96	1.13	Bolt rupture
F2	10	M20 G10.9	22	70	328.64	317.84	0.97	Plate yielding
F3	10	M16 G10.9	18	70	250.16	239.36	0.96	Plate yielding
F4	10	M12 G8.8	14	40	113.80	118.70	1.04	Bolt rupture
E1	20	M12 G8.8	14	40	141	160	1.13	Bolt rupture
E2	10	M20 G10.9	22	70	335	324	0.97	Plate yielding
E3	10	M16 G10.9	18	70	225	244	0.96	Plate yielding
E4	10	M12 G8.8	14	40	116	121	1.04	Inner bolt rupture

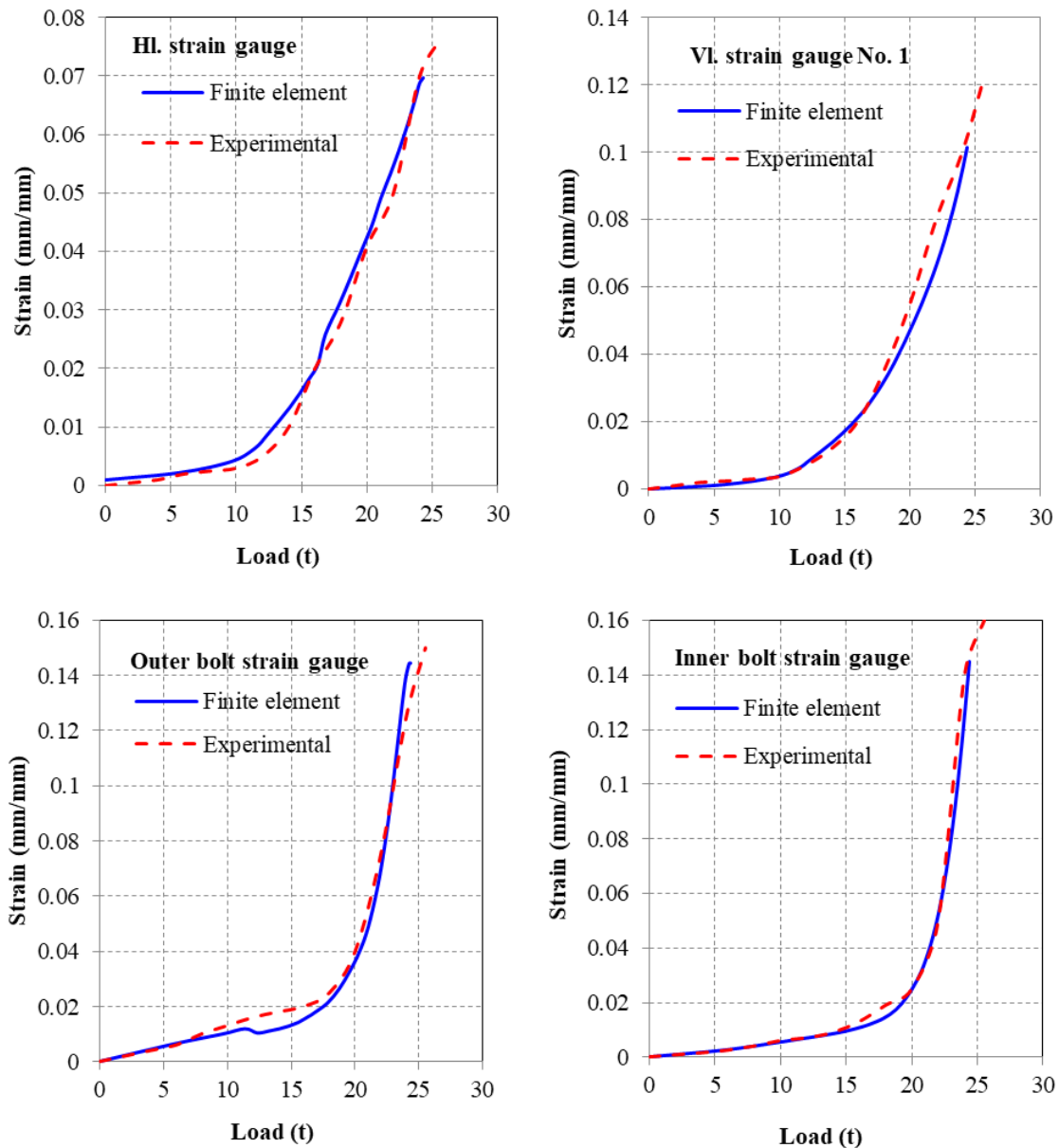


Figure 8. Comparisons experimental and numerical results for Specimen E3.

All connections have two rows of bolts at the tension side, and one bolt row at the compression side with the exception of the 400 mm deep flushed connection where only one row of bolts are used in the tension side. The numerically analysed connections (Figure 9) have the following configurations:

- Flushed end plate with two bolts in one row in the tension side:
 - 400 mm beam depth with 100 mm horizontal distance between bolts.
 - 600 mm beam depth with 100 mm horizontal distance between bolts.
 - 400 mm beam depth with 200 mm horizontal distance between bolts.

- 600 mm beam depth with 200 mm horizontal distance between bolts.
- Flushed end plate with four bolts in two rows in the tension side:
 - 600 mm beam depth with 100 mm horizontal distance between bolts.
 - 600 mm beam depth with 200 mm horizontal distance between bolts.
- Extended unstiffened end plate with four bolts in two rows in the tension side:
 - 400 mm beam depth with 100 mm horizontal distance between bolts.
 - 600 mm beam depth with 100 mm horizontal distance between bolts.

- Extended stiffened end plate with four bolts in two rows in the tension side:
 - 400 mm beam depth with 100 mm horizontal distance between bolts.
 - 600 mm beam depth with 100 mm horizontal distance between bolts.

Analysed connections are denoted by symbols such as 400-F-2-1-100. The first three digits present the beam depth (400 or 600 mm). The second letter indicates a flushed (F) or an extended (E) end plate. The third digit indicates the number of bolts in the tension side with the following one digit indicating the number of bolts' rows (1 or 2). The last two digits indicate the horizontal distance between the bolts (100 or 200 mm). Samples of the numerical analysis results are given herein with full details of these results given elsewhere (Aziz 2010).

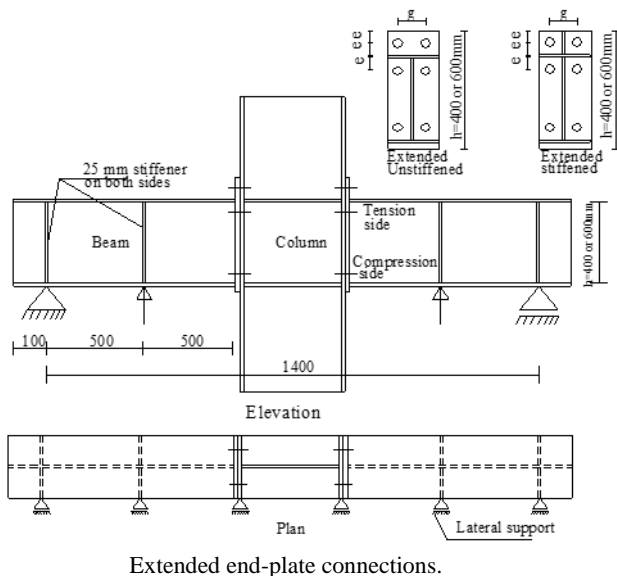
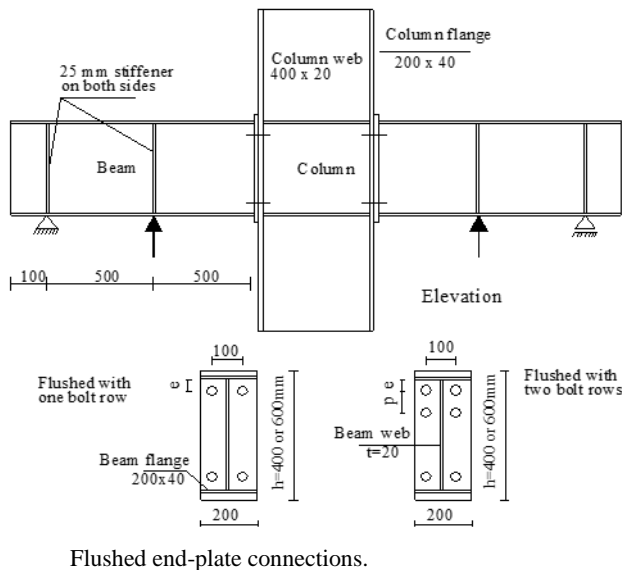
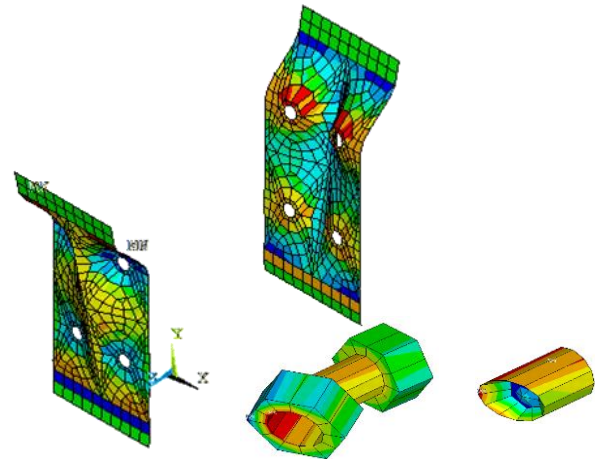


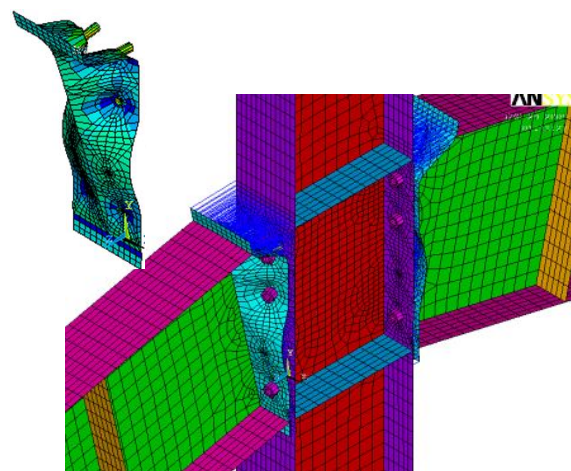
Figure 9. Details of the numerically analyzed flushed and extended end plate connections.

5.1 Flushed End Plate Connections

Two failure modes are recorded in the numerically analysed connections: bolt failure for connections with relatively thick end plates and plate failure for relatively thin end plates connections. For the later one, the force in the tension bolt increases with the increase of the end plate thickness due to the increase of the plate resistance. For relatively thick end plates, where failure turns to be in the bolts, the tensile forces in these bolts increase although the moment capacity of the connection remains constant. The axial force in any bolt does not reach its nominal resistance. This is because the bolt shank rotates with the end plate; and as such, the bolt is subjected to a bending moment beside the axial tension (Figure 10). Thus, the bolts suffer a combination of axial tensile force and flexure, especially for thin end plates, which exhibit large deformations.



10 mm thick end plate and bolt deformation for 400-F-2-1-100 connection with M24 bolts



Deformed shape of connection 600-F-4-2-100 with 10 mm plate thickness and M24 bolts

Figure 10. Sample of the deformed shape of the numerically analyzed flushed end plate connections.

For connections with relatively thick end plates and relatively small bolt diameters, small deformation of the end plate is recorded and hence, no bolt's rotation is encountered; consequently, bolts are only subjected to axial tensile force. For connections with two rows of bolts and relatively thick end plates, forces in outer bolts are always larger than those in the inner bolts as the plate rotates as a rigid body without noticeable deformation. The centre of rotation is found to be at the centre line of the beam compression flange.

Figure 11 presents samples of the results for the moment capacity of the analysed flushed end plate connections. Regardless of the end plate thickness, it is found that the larger the edge distances the smaller the moment capacity of the connection. Each curve of Figure 11 can be divided into two main segments: the first segment represents end-plate failure where the moment capacity increases linearly with the increase of the plate thickness while the second segment represents bolt rupture where the moment capacity is almost constant. For connections with M12 bolts and one bolt row, the first segment of the curve nearly does not exist because bolt diameter is small enough to maintain connection failure by bolt rupture even for thin end plates. Figure 11 also shows the variation of the connection moment capacity for a certain edge distance ($e = 3.0 d$) with changing other parameters. It is evident that for thin end plates, and despite having a failure mode governed by plate failure, the bolt diameter still has a significant effect on the connection moment capacity since the increase in the bolt's resistance decreases the end plate deformations. For thicker end plates, the ratio between ultimate moments for each bolt diameter is nearly the same as the ratio between the bolts' areas, while for thin end plates, the previous observation is not valid.

5.2 Extended End Plate Connections

Generally, the increase in the end plate thickness increases the connection moment capacity. Samples of the deformed shapes for unstiffened and stiffened end plate connections are shown in Figure 12.

The 10 mm thick unstiffened end plate of connections with M24 bolts suffers bending moments in two directions (biaxial moment), while the 20 mm thick end plate experience almost a uniaxial bending moment. When the head plate thickness increases to 40 mm, a very small deformation is encounter in the plate. Thus, it can be concluded that the smaller the thickness of the end plate, the larger its deformation.

Furthermore, smaller bolt diameter results in smaller end plate deformations with failure tends to be in the bolt. For larger bolt diameters, the bolt becomes strong enough to maintain its undeformed shape and most of the deformation occurs in the end plate.

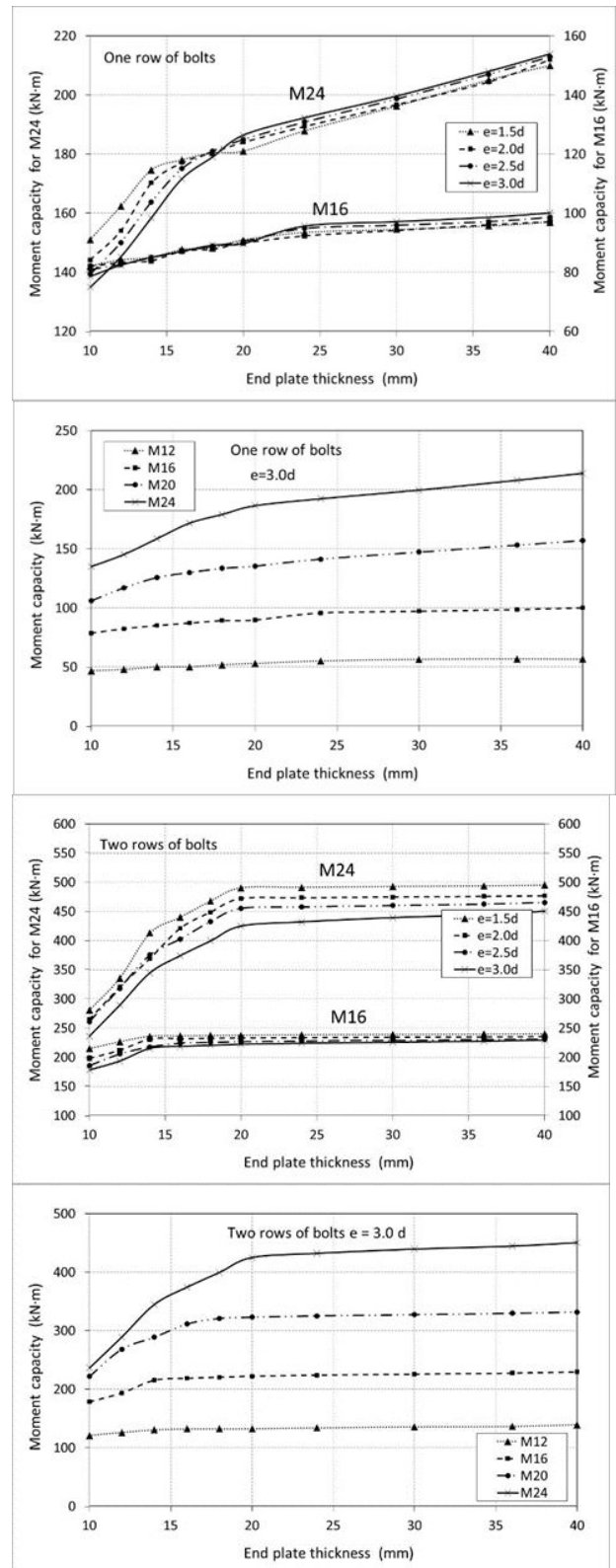
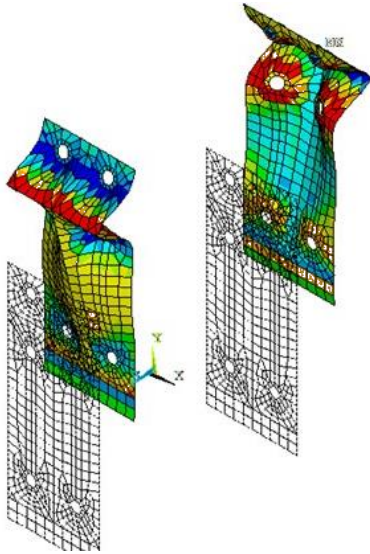
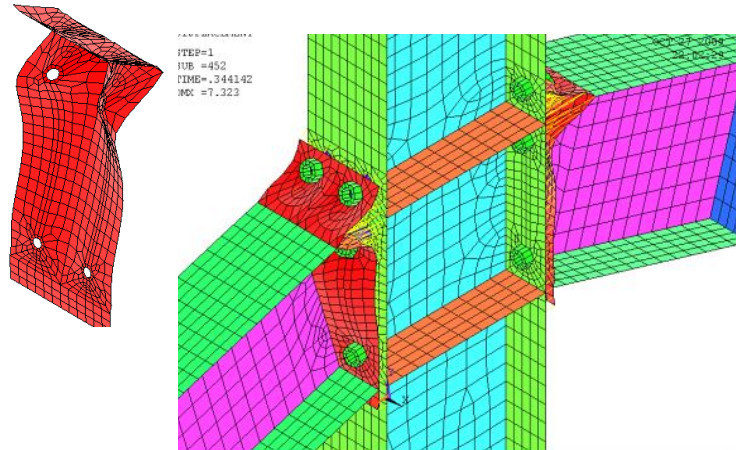


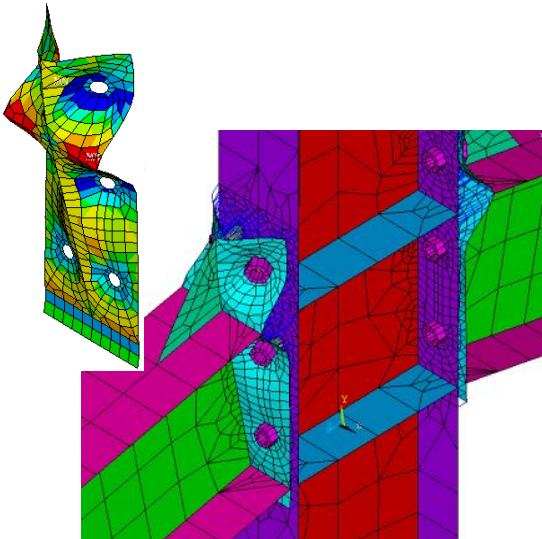
Figure 11. Moment capacity for the numerically analysed flushed end-plate connections with one and two rows of bolts in the tension side.



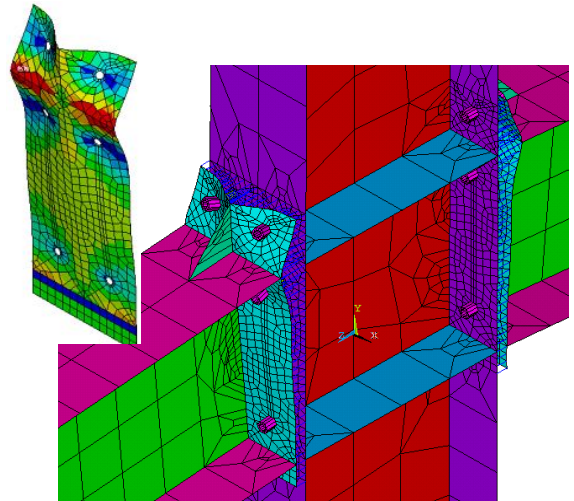
20 mm thick unstiffened end plate deformation for 400-E-4-2-100 connection with M24 bolts.



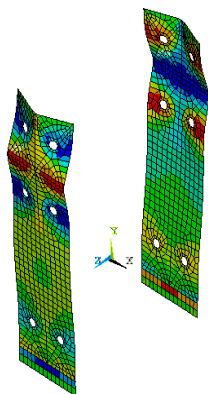
Deformed shape of connection 400-E-4-2-100 with 10 mm plate thickness and M24 bolts and unstiffened end plate.



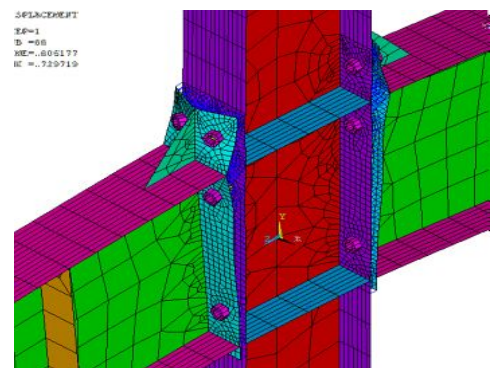
10 mm thick stiffened end plate and bolt deformation for 400-E-4-2-100 connection with M24 bolts



20 mm thick stiffened end plate and bolt deformation for 400-E-4-2-100 connection with M24 bolts and stiffened end



10 mm thick stiffened end plate deformation for 600-E-4-2-100 connection with M24 bolts



Deformed shape of connection 600-E-4-2-100 with 10 mm plate thickness and M24 bolts and stiffened end plate

Figure 12. Sample of the deformed shape of the numerically analyzed extended stiffened and unstiffened end plate connections.

For stiffened end plate connections, the stiffness of the extended portion of the plate significantly increases and consequently, its deformation decreases.

Thus, for connections controlled by plate failure, the connection moment capacity increases. The deformed shapes of both stiffened and unstiffened

connections are found to be almost the same for connections with thick end plates. Samples of these deformed shapes for stiffened end plate connections are shown in Figure 12. The portion in the extended part above the beam flange works as two-way plate supported on both the beam flange and the stiffener. This gives large stiffness to the plate and decreases its deformations and increases the moment capacity of connections with relatively thin end plates, which are controlled by plate failure.

Samples of the relationship between the end plate thickness and the connection moment capacity are presented in Figure 13, which reveals an almost bi-linear relation. Once again, the first segment of the curve (in case of relatively thin end plates) represents the plate failure mode. In this segment, the connection's moment capacity increases noticeably with the increase of end plate thickness. The second segment of the curve (in case of relatively thick end plates) represents bolt rupture failure mode. In this segment, the connection's moment capacity slightly increases with the increase of the end plate thickness. This is attributed to a reduction of the end plate deformation and consequently, a reduction in the additional bending moment affecting the bolt shank.

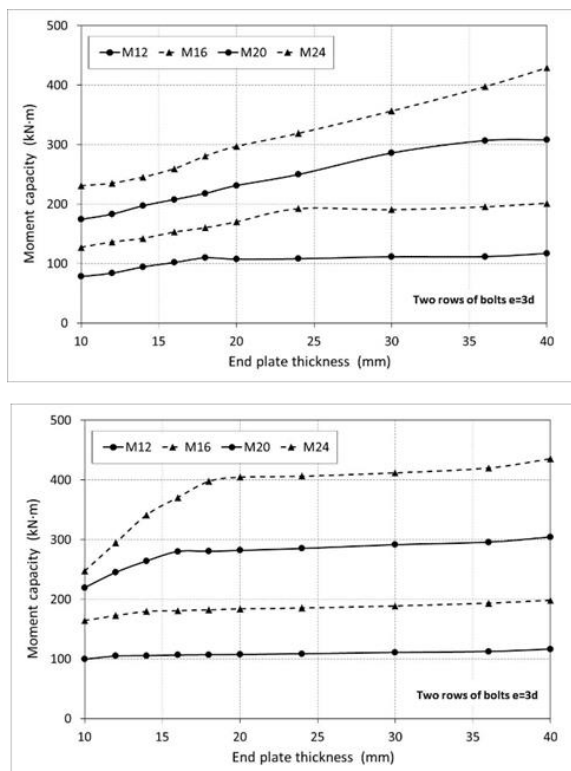


Figure 13. Moment capacity of connections with unstiffened (above) and stiffened (below) end-plates.

Figure 13 also shows that for extended unstiffened connection with relatively thin end plates, although the mode of failure of these connections is governed by plate failure, bolt diameter significantly affects

the moment capacity of the connection. This is because the increase in the bolt resistance actually acts to decrease the plate deformation, which increases the connection resistance. Connections with thicker end plates, where the moment capacity depends on the bolt strength, the ultimate force in each bolt is almost proportional to its cross-section area. On the other hand, for thin end plate connections, the connection capacity is controlled by the plate strength and the previous observation is no longer valid. The numerical analysis also reveals that the force in the outer bolt is greater than that in the inner one for connections with relatively thick end plates (16 mm or more).

Figure 13 also presents the relationship between the end plate thickness and the moment capacity of the stiffened connection. The figure reveals an increase in the moment capacity of connections having M24 and M20 bolts up to a certain end plate thickness. On the other hand, for connections with M16 and M12 bolts, the moment capacity is nearly constant for different end-plate thicknesses. This is because, for smaller diameter bolts, failure always occurs in the bolt. This behaviour is not pronounced for unstiffened connection, which reveals that the stiffener prevents plate yielding for connections with small diameter bolts. Similar to unstiffened end plate connections, the analysis also reveals that for connections with thick end plates (16 mm thickness or more), the force in the outer bolt is greater than that in the inner bolt.

For connections having relatively thin unstiffened end plate and large bolt diameter, the plate behaves elastically in both directions and the prying forces (Figure 14) appears at three locations: high value at the upper edge of the end plate, and very low values at the bolts just below the beam's tension flange and in the vicinity of the compression zone. In case of relatively thick end plate, the plate is rigid enough to deform only in the vertical direction and prying forces are recorded only at the top edge of the plate. Figure 14 also presents the relation between the end plate thickness and the prying force for beam's height of 400 mm and edge distance $e = 3d$. It is evident from this figure that the prying force increases with the increase in the end plate thickness up to a certain value at which the prying force begins to decrease till it reaches zero. This value is almost the same border value that separates plate and bolt failure modes in connections.

For stiffened connections with relatively thin end plates, prying force appears in the same three locations described above for unstiffened specimens.

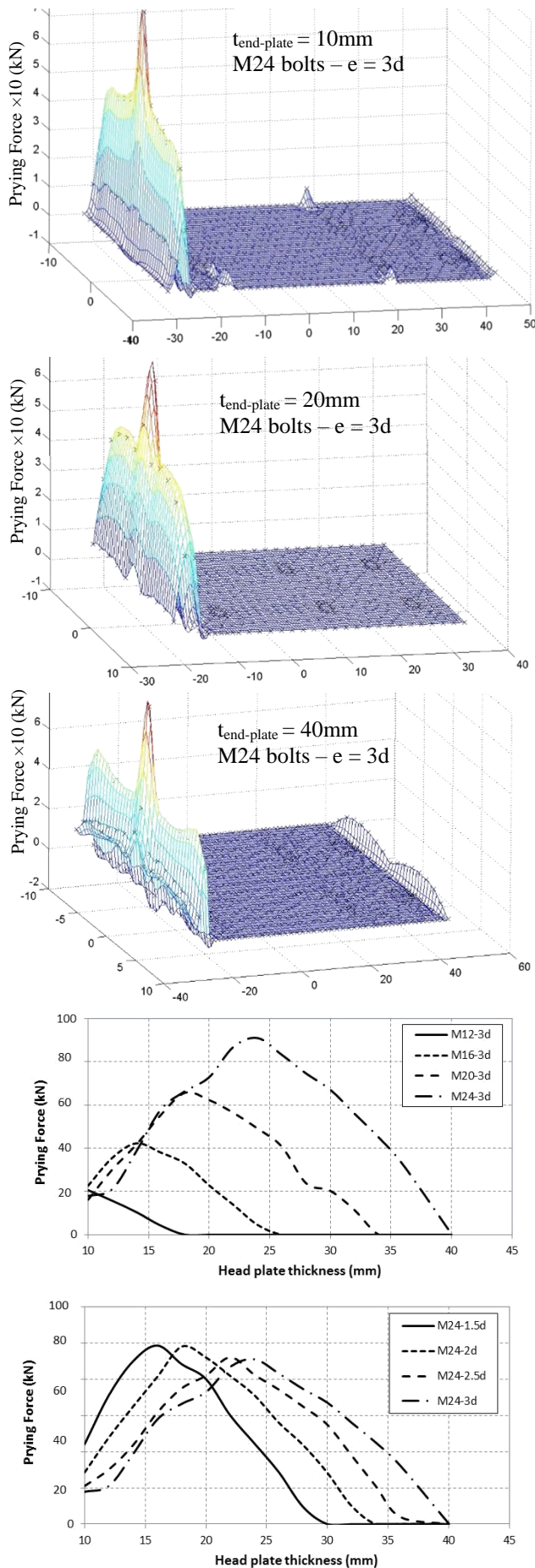


Figure 14. Prying force for different end plate thickness and for beam height = 400 mm.

However, the prying force in the extended part turns out to be in the plate corners instead of being visible along the whole width of the plate. Increasing the end plate thickness eliminates the prying force at bolts that lie below the beam flange, while it still appears in zones of the outer bolts above the flange. For connections having relatively thick end plates, prying forces are found to be significantly small and can be neglected. Thus, it can be generally concluded that the ratio of the prying force to the tensile bolt force decreases by the increase of the end plate thickness for different bolt diameters and edge distances.

6 NUMERICAL ANALYSIS RESULTS VERSUS AISC DESIGN GUIDE PROVISIONS

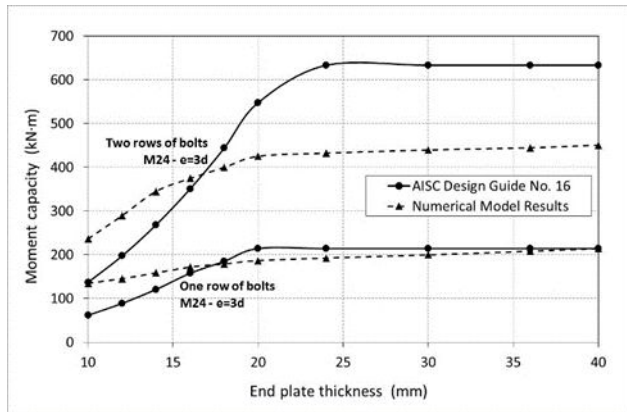
Figure 15 shows a typical sample of the comparative study performed on the flushed end plate connections' capacities resulting from the numerical analysis and those obtained by following the AISC design guide no. 16 provisions. The AISC provisions assume that there is no induced prying force except when the stress in the plate reaches 90% of its yield strength. It is evident from Figure 15 that the AISC provisions overestimate the capacity of a connection that fails by bolt rupture and underestimate it for a connection that fails by plate yielding.

The discrepancy between results of the AISC provisions and numerical analysis outcomes for connections failing by bolt rupture is attributed to the fact that the AISC provisions neglect the additional bending moment affecting the bolt due to the end plate rotation, which is referred to in this paper as the interaction between the plate deformation and bolt elongation. It is worth mentioning that increasing the end plate thickness reduces its deformation and the bolt's rotation, which leads to an increase in the ability of the bolt to resist the tensile force acting on it and vice versa.

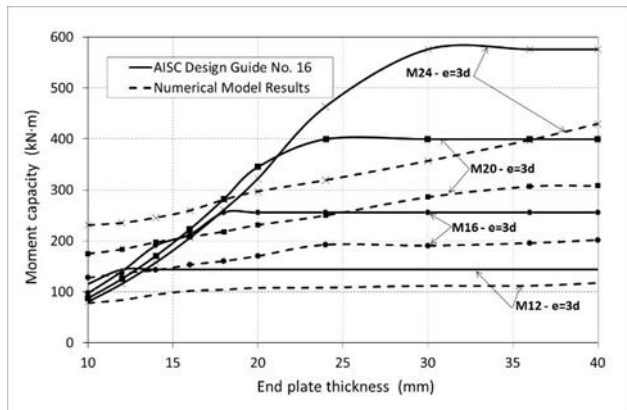
On the contrary, for connections failing by plate yielding, the AISC provisions consider the bolt as an infinitely rigid support neglecting its elongation: applying the yield line analysis to the end plate, should not only consider the internal work due to plate deformation but also that due to the bolt's elongation. Thus, the discrepancy between the AISC provisions and the numerical analysis results increases with the increase in bolt diameter.

Figure 15 also shows another typical sample of this comparative study performed on extended end plate connections with M12 to M24 bolts. For M12

connections, the AISC provisions overestimate the connection capacity. For M16 to M24 connections, the AISC design provisions overestimate the connection capacity for connections failing by bolt rupture and underestimate it for those failing by plate yielding. The same conclusions and observations mentioned above for flushed end plate connections is also applicable to the extended end plate connection behaviour.



Flushed end plate connection.

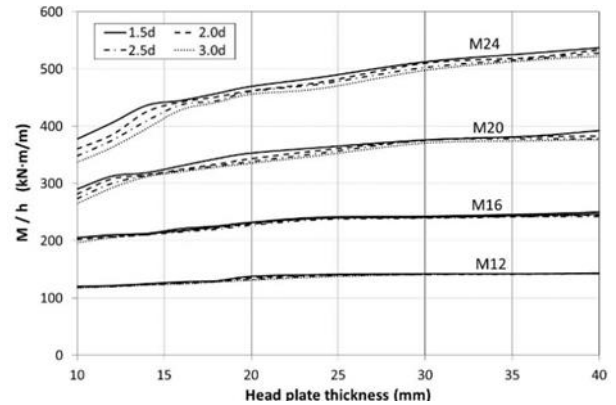


Extended end plate connection.

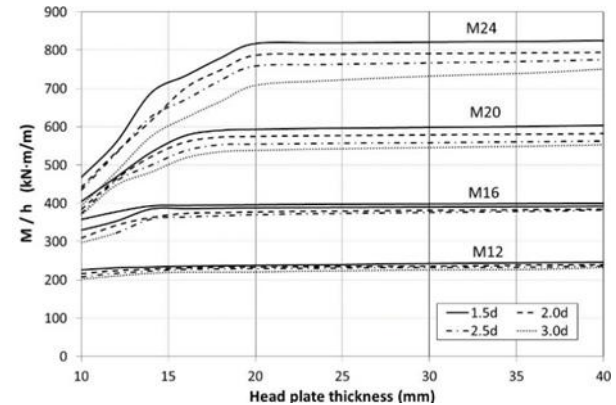
Figure 15. Comparison between numerical analysis results of and AISC Design Guide No. 16 outcomes.

7 DESIGN RECOMMENDATIONS

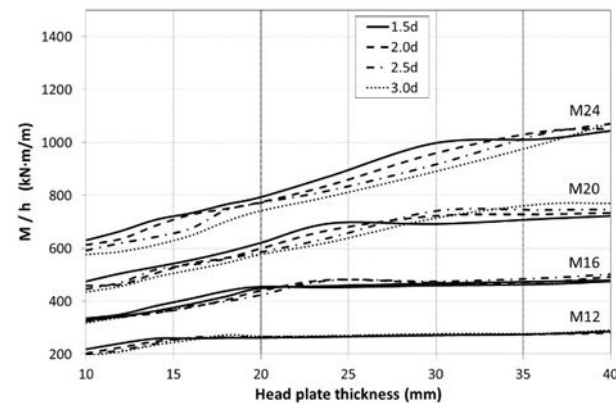
The results of the numerical analysis are used to build a series of design charts for the capacity of the investigated connections (Figure 16). The charts provide an effective, easy and accurate technique to choose the bolt diameter and the corresponding end plate thickness for a given moment capacity M and beam height h ; the moment capacity in these charts is related to the beam height (M/h) which results in the equivalent tension force in the tension flange. The effects of the prying force, the bolt elongation, the bolt rotation and the head plate deformation are all included in these charts.



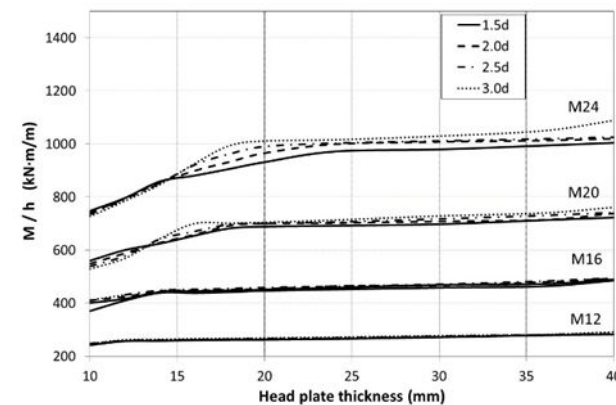
Flushed end plate connections with one row of bolts.



Flushed end plate connections with two rows of bolts.



Extended unstiffened end plate connection



Extended stiffened end plate connections

Figure 16. Design charts capacity of flushed and extended end plate connections.

Furthermore, a semi-graphical design aid is developed where the connection's capacity M is calculated as follow

$$M = \min \begin{cases} M_{plate} = 0.01(c_1 + c_2 t_p) F_{yp} h^2 g \\ M_{bolt} = 0.01(c_3 + c_4 t_p) F_{yb} h^2 g \end{cases} \quad (1)$$

where F_{yp} and F_{yb} are the yield stress of the end plate and the bolt, respectively, h is the beam height and g is the horizontal distance between the bolts. Four curves are plotted (Figures 17 and 20) to determine the constants c_1 to c_4 based on a regression analysis (Aziz 2010) performed on the data numerically obtained.

9. CONCLUSIONS

The current paper presents an experimental and numerical investigation performed on steel rigid I-beam to column bolted connections with flushed and extended end plates. The analyses reveal two distinct failure modes for these connections. For thin end plate, the connection's capacity is mainly governed by plate failure while for thick end plate, failure of bolts controls the connection's capacity. Furthermore, the investigations show that bolts of thin end plates connections are subjected to biaxial bending resulting from the excessive plate deformation. For thick plates, the connection capacity is almost proportional to the bolts cross-section area.

For unstiffened connections with extended thin end plate, prying force appears beside both the inner and outer bolts. On the other hand, this prying force appears only at the position of outer bolts for moderately thick end plate connections. For connections with thick end plate, the prying force almost vanishes. The addition of stiffener to the extended end plate connections considerably decreases the prying force and the position of the prying force turns to be in plate corners instead of being at the outer edge for extended unstiffened end plate connections. For thin extended end plate connections, the moment capacity of the connection without a stiffener is generally less than that with a stiffener. For thick extended end plate, the moment capacities of both stiffened and unstiffened connections are almost the same.

The analyses also show that AISC design guide no 16 provisions overestimate the connection capacity for connections failing by bolt rupture and underestimate it for connections failing by plate failure. Based on the outcomes of the numerical analysis, design charts and equations for rigid end plate connections are developed. These design aids enable the

designer to calculate the connection capacity for specific bolt diameter, edge distance, and end plate thickness without performing complicated and lengthy calculations as currently adopted by most codes of practice.

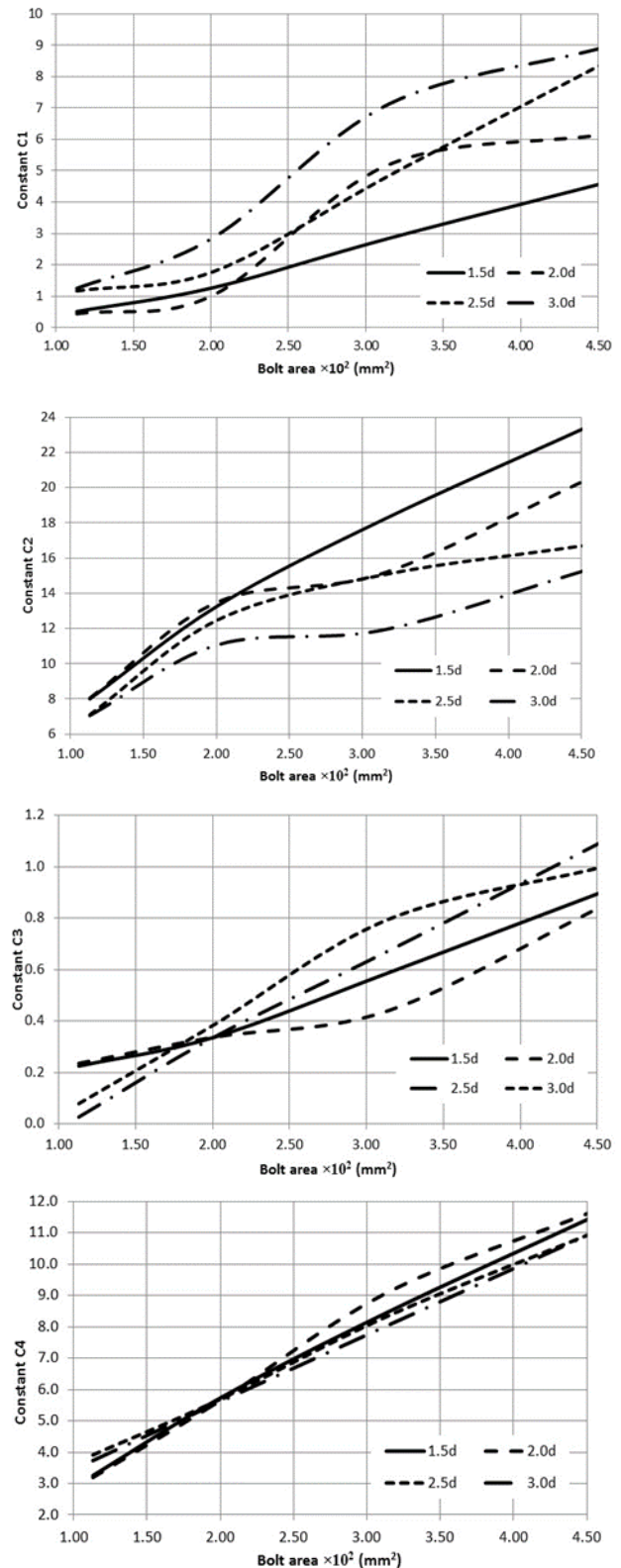


Figure 17. Factors c_1 to c_4 adopted to estimate flushed end plate connection capacity with two bolts in the tension side.

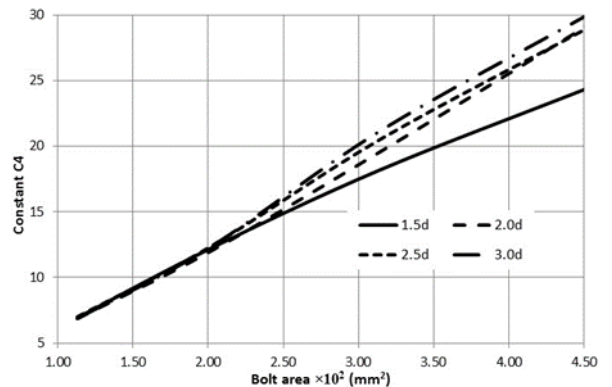
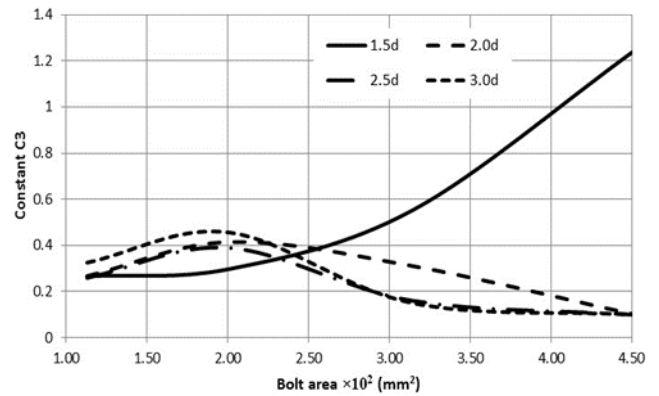
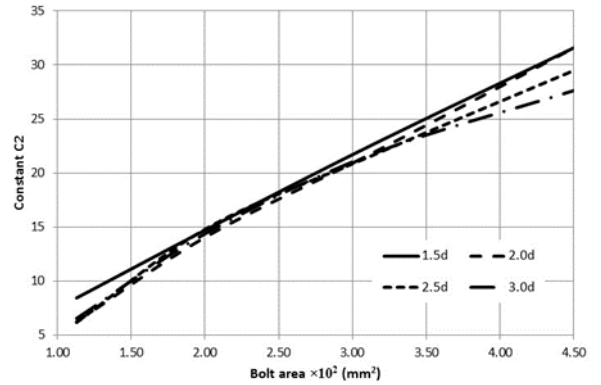
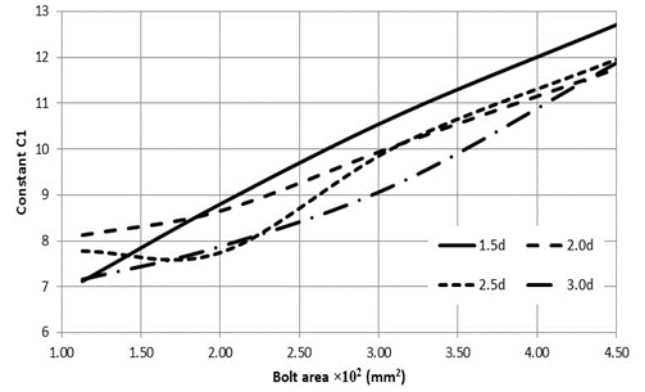
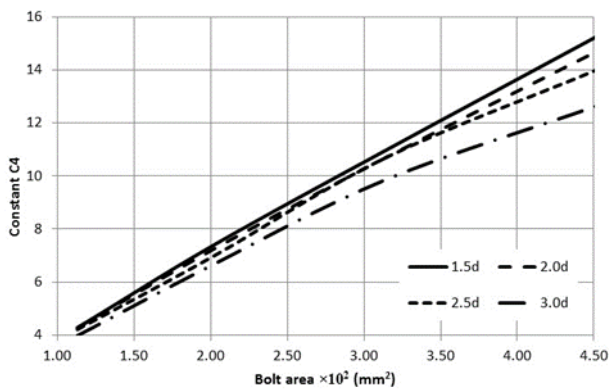
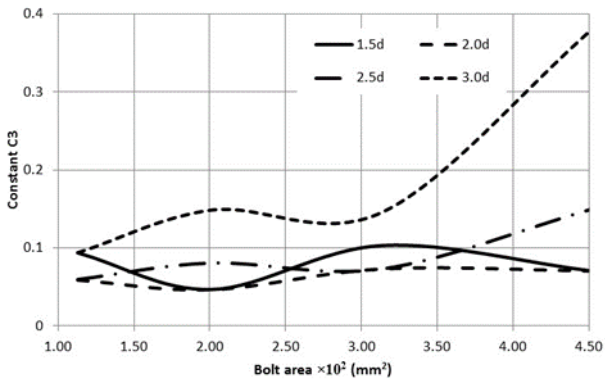
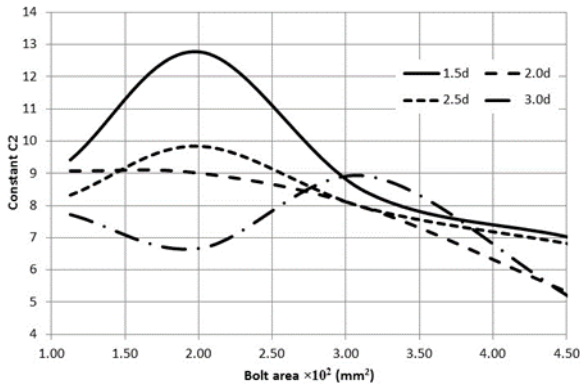
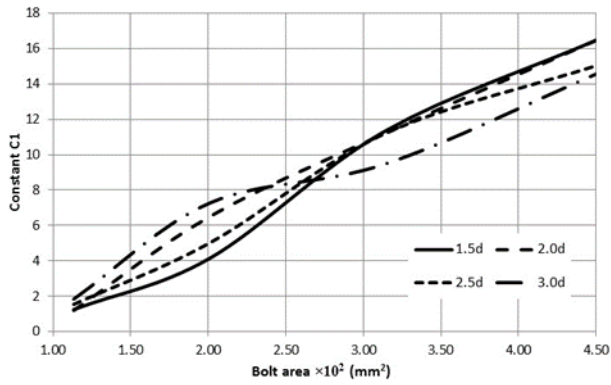


Figure 18. Factors c_1 to c_4 adopted to estimate flushed end plate connection capacity with four bolts in the tension side.

Figure 19. Factors c_1 to c_4 adopted to estimate unstiffened extended end plate connection capacity with four bolts in the tension side.

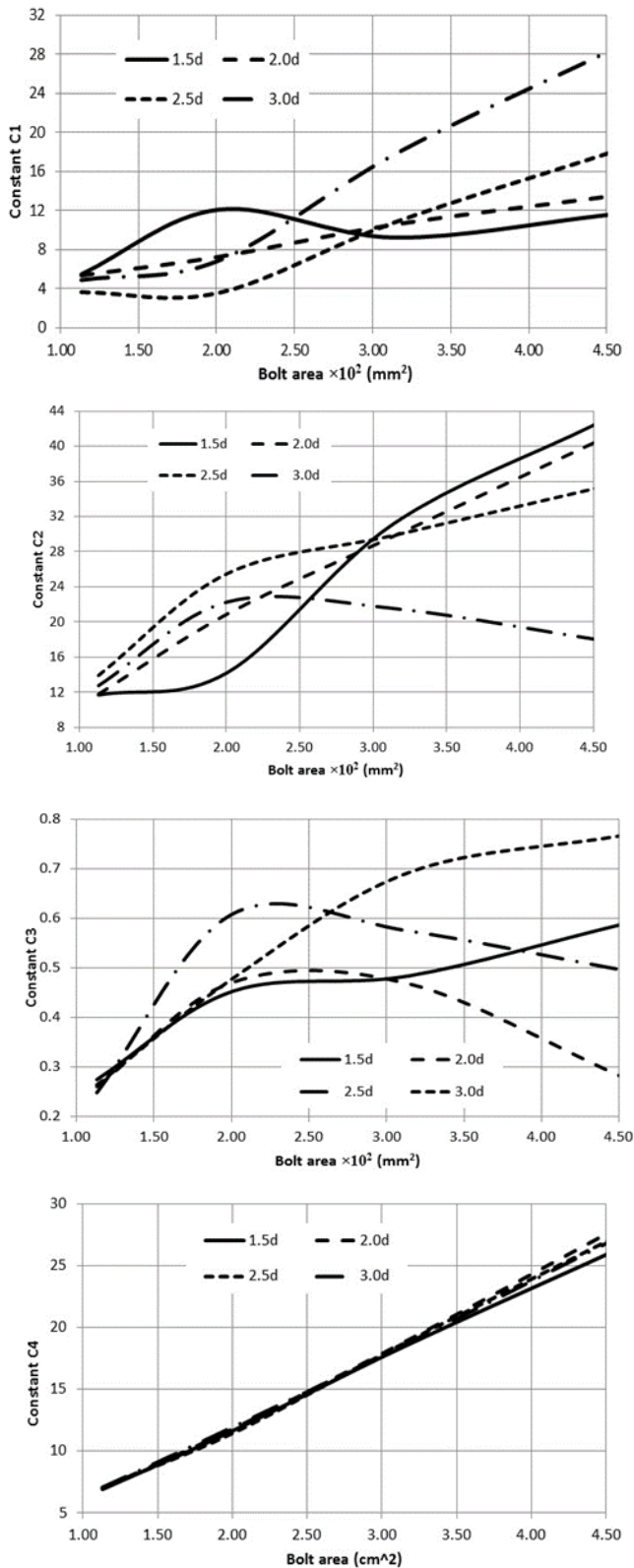


Figure 20. Factors c_1 to c_4 adopted to estimate stiffened extended end plate connection capacity with four bolts in the tension side.

8 REFERENCES

American Institute of Steel Construction. Extended end plate moment connections. Steel design guide No16. Chicago, USA. 1990

Aziz, R. Behavior and Design of Steel I-beam-to-Column Rigid Bolted Connections, PhD dissertation, Structural Eng. Dept., Faculty of Engineering, Ain Shams University, Cairo, Egypt. 2010.

Bose, B., Youngson, G. K., and Wang, Z. M. An appraisal of the design rules in Eurocode 3 for bolted end-plate joints by comparison with experimental results. Proceedings of the Institution of Civil Engineers-Structures and Buildings, 1996, 116(2), 221-234.

Bursi, O. S., and Jaspart, J. P., Calibration of a finite element model for isolated bolted end-plate steel connections, Journal of Constructional Steel Research, 1997, 44(3), 225-262.

Coelho, A. M. G., and Bijlaard, F. S., Experimental behaviour of high strength steel end-plate connections”, Journal of Constructional Steel Research, 2007, 63(9), 1228-1240.

Diaz, C., Victoria, M., Martí, P., and Querin, O. M., FE model of beam-to-column extended end-plate joints”, Journal of Constructional Steel Research, 2011, 67(10), 1578-1590.

Grimsmo, E. L., Clausen, A. H., Langseth, M., and Aalberg, A., An experimental study of static and dynamic behaviour of bolted end-plate joints of steel, International Journal of Impact Engineering, 2015, 85, 132-145.

Ismail, R. E., Fahmy, A. S., Khalifa, A. M., and Mohamed, Y. M., Behavior of end-plate steel connections stiffened with stiffeners of different geometrical dimensions”, Global Advanced Research Journal of Engineering, Technology and Innovation, 2014, 3(3), 55-69.

Jenkins, W. M., Tong, C. S., and Prescott, A. T., Moment-transmitting endplate connections in steel construction, and a proposed basis for flush endplate design, Structural Engineer. 1986, Part A, 64, 121-32.

Krishnamurthy N., A fresh look at bolted end-plate behavior and design, Engineering Journal, 1978, 15(2), 39 – 49.

Mann, A.P., Plastically designed endplate connections, PhD Thesis, University of Leeds, UK. 1968.

Murray, T. M., and Shoemaker, W. L., Flush and Extended Multiple-Row Moment End-Plate Connections. Steel design guide series 16, American Institute of Steel Construction. Chicago, IL, USA. 2002.

Packer, J. A. and Morris, L. J., A limit state design method for the tension region of bolted beam-column connections, The Structural Engineer, 1977, 55(10), 446 – 458.

Sherbourne, A. N., and Bahaari, M. R., 3D simulation of end-plate bolted connections, Journal of Structural Engineering, 1994, 120(11), 3122-3136.

Shi, G., Chen, X., and Wang, D., Experimental study of ultra-large capacity end-plate joints, Journal of Constructional Steel Research, 2017, 128, 354-361.

Srouji, R., Kukreti, A. R. and Murray, T. M., yield-line analysis of end-plate connections with bolt force predictions, Research Report FSEL MBMA 83 – 05, Fears Structural Engineering Laboratory, University of Oklahoma, USA. 1983.

Tarpy Jr., T.S. and Cardinal J.W., Behaviour of semi-rigid beam-to-column end-plate connections, Proceedings of the Int. Conf.: Joints in Structural Steel Work, Teesside Polytechnic, Cleveland, England, April 6-9, 1981, pp. 2.3-2.25.

Wang, T., Wang, Z., Wang, J., and Feng, J., A simplified calculation model for moment-rotation curve used in semi-rigid end-plate connections. Journal of Information and Computational Science, 2013, 10(11), 3529-3538.

Zoetemeijer, P., Semi-rigid bolted beam-to-column connections with stiffened column flanges and flush-end-plates, Joints in Structural Steelwork, Pentech, London, 1981, 2.99 – 2.118.